SAND CASTING OF SURFACE ALLOYED BUTTERFLY VALVE WITH IMPROVED HARDNESS AND CORROSION RESISTANCE BY INCORPORATING METAL POWDERS IN-MOLD COATINGS

Kaustubh Rane, Michael Beining, Swaroop Behera, and Pradeep Rohatgi
Department of Materials Science and Engineering, University of Wisconsin-Milwaukee, Milwaukee, WI, USA

Amir Kordijazi
Department of Materials Science and Engineering, University of Wisconsin-Milwaukee, Milwaukee, WI, USA
Department of Industrial and Manufacturing Engineering, University of Wisconsin-Milwaukee, Milwaukee, WI 53211, USA

Ajay Kumar
Department of Materials Science and Engineering, University of Wisconsin-Milwaukee, Milwaukee, WI, USA
Department of Mechanical Engineering, Indian Institute of Technology, Tirupati, AP, India

Copyright © 2021 American Foundry Society
https://doi.org/10.1007/s40962-021-00609-4

Abstract

A cost-effective procedure to surface alloy WCB steel butterfly valve sand castings using mold coatings incorporating metal and ferroalloy powders has been described. The tooling, mold design, and casting conditions similar to plain WCB castings were successfully used to produce sound surface alloyed butterfly castings under industrial conditions. The surface alloying was achieved by adding powders of Ni, Cr, Fe–Si, Fe–Mn, and Mo to the slurry containing a binder coated on the mold surface. The surface alloyed coatings on the surface of WCB steel butterfly valve castings were enriched in Ni, Cr, Mo, and Mn up to 6.4, 23.2, 3.3, and 1.1%, respectively. The depths of coatings were as high as 420 μm. After normalizing and tempering heat treatment, the surface alloyed layer exhibited an increase in corrosion resistance as compared to base metal WCB steel.

Keywords: *surface alloying, corrosion, austenite phase, heat treatment, butterfly valve, nickel, chromium, manganese, silicon, molybdenum*

Introduction

Many metallic components used in applications involving exposure to the corrosive aqueous and atmospheric conditions suffer from the degradation of the surface. The degradation can result in the form of corrosion and wear of the surface. These problems are especially widespread for castings that are utilized in the water supply industry, including pumps, butterfly valves, valve seats, faucets, and flanges. To prevent corrosion on the surface of these components, water industries rely on coatings or using casting stainless steel components on account of their corrosion-resistant properties.[1] Since corrosion is a surface phenomenon, mainly the surface of components needs to be corrosion resistant as compared to the core of the material, and therefore, surface alloying techniques can be applied to change the composition of surface in order to improve corrosion resistance.

This is an updated version of the paper presented during the 125th AFS Metalcasting Congress and published in 2021 AFS Transactions (K. Rane, M. Beining, S. Behera, A. Kordijazi, A. Kumar, P. Rohatgi, Sand casting of surface alloyed butterfly valve with improved hardness and corrosion resistance by incorporating metal powders in-mold coatings. AFS Trans. 129, 1-11 (2021)).

Received: 17 February 2021 / Accepted: 27 March 2021
Published online: 04 May 2021

Various surface alloying techniques have been reported in the literature. Jiang et al. performed surface alloying of multi-element Ni–Cr–Mo–Cu surface alloyed layer on low-carbon steel and AISI 304 stainless steel materials using a double glow plasma process.[2] It was observed that the relative content of Cr_2O_3 in the passive film of the alloying layer formed on the 304 stainless steel is 3.75% more than that in the passive film of the alloying layer formed on the low-carbon steel, and this corrosion-resistant film was in favor of the corrosion resistance. Majumdar et al. investigated the effect of (WC + Ni + NiCr) used as a corrosion-resistant alloying powder that was applied on the surface of AISI 304 stainless steel by laser surface alloying process.[3] The microhardness of the alloyed zone was significantly improved to a maximum value of 1350 VHN as compared to 220 VHN of as-received γ stainless steel. Krishnakumar and Srinivasan used gas tungsten arc for surface alloying stainless steel with titanium and tungsten,[4] and Fals et. al. used laser surface alloying on flame prayed NbC coatings on a stainless steel substrate.[5] Jeyaprakash et al used laser cladding to add nickel and cobalt coatings on stainless steel substrates.[6] Amirsadeghi and Sohi studied the surface melting of austempered ductile iron using the TIG process with molybdenum and chromium as alloying elements that leads to the formation of a hardened alloyed layer.[7]

Surface enrichment by ball milling is an alternate technique used to improve the pitting corrosion resistance of stainless steel. 316L stainless steel is enriched with approximately 18% Cr, which helps to prevent surface corrosion, but the addition of Mo can help to prevent pitting corrosion as well.[8] Electric discharge surface alloying has been conducted with a chromium anode where in an electric arc produced by the anode lead to rapid melting and solidification of chromium on the surface of low-carbon steel.[9] The surface of 304 as a substrate has been laser clad with 316L stainless steel and WC powders using a 700 W laser to form a surface with improved hardness.[10] Cao, et.al., used a mixture of V, Cr, Ti, and Mo which was applied to the surface of the substrate which was alloyed using a high temperature plasma arc with a maximum energy density of 10^6 W/cm^2.[11] All of these processes showed major improvements in the properties of the substrate, but they are mostly expensive methods and cannot be applied on large components as needed in water distribution system.

Surface alloying by casting is a good solution to impart high local wear and corrosion resistance to cheaper and common industrial materials. The idea of surface alloying of mild steel was first patented in 1969 by the International Nickel Company.[12] The process was developed to surface alloy gray iron, alloy cast iron, and alloy ductile iron with nickel and chromium-containing metallic powders, and other nickel alloy powders.

Some of the main characteristics of surface alloying during casting include: (1) the surface properties of materials and parts can be tailored to specific requirements (resistance against corrosion, wear, oxidation); (2) the alloyed layer is metallurgically bonded to the base metal; and (3) surface finish can be controlled, and machining allowance can be provided. Ni and Cr are the frequently used alloying elements for improving the performance of various iron alloys such as the wear resistance, corrosion resistance, and thermal resistance. Ni can dramatically improve the chemical stability of the iron alloys so as to increase their corrosion resistance. Cr leads to the formation of an oxide layer, which is highly protective against corrosion reaction.

In the present study, we developed targeted multi-element Ni, Cr, Fe–Mn, Fe–Si, and Mo enriched surface alloyed layer coatings on the WCB steel butterfly valve on industrial scale using gravity sand casting process for improving its hardness and corrosion resistance properties. These elements for enrichment were picked since they are present in super duplex stainless steels, which have very high corrosion resistance. A butterfly valve is a quarter-turn rotational motion valve, which is used to stop, regulate, and start the flow. This valve can be used in many different fluid services such as cooling water, air, gases, and fire protection; slurry and similar services; vacuum service; and high-pressure and high-temperature water and steam services. Characterization of the microstructures and phases in the surface alloyed layer has been carried out to understand the effect of process parameters. Microhardness and corrosion resistance have been measured.

Experimental Procedure

Casting Procedure

The industrial butterfly valves casting molds (Figure 1) were obtained from an industrial foundry (hereby referred to as the industry) to demonstrate surface alloying. Figure 1a, c shows pictures of the actual molds. The molds were made from 80-grain fineness silica sand. A phenolic urethane organic binder system (binder level ~1.2%) was used to ensure good gas permeability and surface finish during casting. The catalyst used was set to allow for an 8–10-minute work-strip time. The sand and binder/catalyst chemicals were mixed in an Omega Tinker industry mixer and then dumped onto the pattern. The sand was manually smoothed, as well as with a strike-off bar, and allowed to set for 10 minutes. After the curing was complete, and the mold halves were extracted from the pattern by flipping inversion of the pattern using a manipulator crane. The mold cavities were coated with a refractory wash (REFCOTEC REFCOHOL 1010) to avoid any reaction between the molten metal and the sand. After applying binder and surface alloying elements on mold and allowing the slurry to dry and harden (Figure 1b, d), the molds were closed, and a zircon filter was placed in the down sprue of the mold.

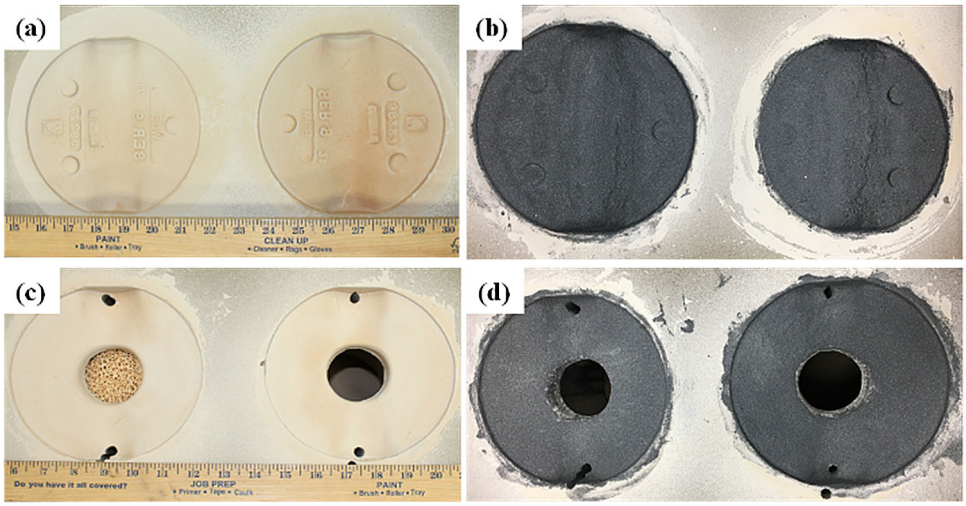

Figure 1. Butterfly valve molds for industrial casting. (a, c): Bare and cleaned surface coated with zircon; (b, d): multi-element powder-coated mold surface using sodium polyacrylate.

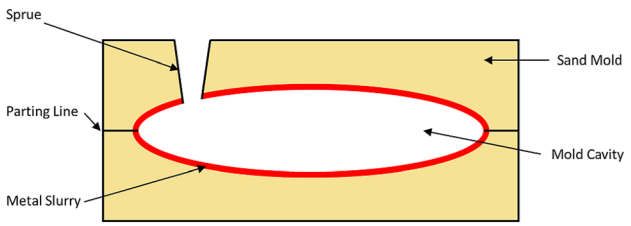

Figure 2. Schematic diagram of the sand mold with the alloying powder slurry applied on the inner surface of the mold cavity. The alloying slurry is a combination of the alloying powders and the binder medium.

Then, three samples were made using two different techniques. The first two samples were prepared by adding the Ni and Cr powders onto a wet refractory wash coating, and the third sample was made using a slurry containing Ni, Cr, Fe–Mn, Fe–Si, and Mo mixed with sodium polyacrylate (NaPA) binder. Figure 2 shows a schematic representation of the sand mold before the WCB steel melt is poured. Once the mold surfaces were coated, they were sealed using SonicSTIK®—core and mold adhesive. The molds were then transported back to the industrial foundry for casting. Once the castings had been poured, they were shaken out and shot blasted with steel shots, and risers and gating were cut off at the industry and were then transported back to the laboratory for analysis.

Figure 3 shows a commercially available butterfly valve, and the surface alloyed butterfly valve prototypes cast at the industrial foundry in the present study. The objective was to quantify the levels of enrichment that could be achieved in an industrial setting for casting a component which requires high quantities of alloying elements on the surface for wear and corrosion resistance. The chemical composition of the WCB base alloy is presented in Table 1. Table 2 presents the composition of the alloying elements used for the surface alloying of the industrially cast butterfly valves.

Figure 3. (a) A commercially available butterfly valve, (b) surface alloyed butterfly valve prototypes cast at the industrial foundry and UWM.

Table 1. Elemental Composition of WCB Steel from Experimental Heat

Element	C	Mn	P	S	Si	Fe
Weight%	0.22	0.84	0.021	0.019	0.41	Balance

Metallographic Preparation

Surface alloyed cast samples were cut and metallographically prepared. The samples were carefully ground with SiC abrasive papers through 120 grit followed by 9 μm diamond suspension, 3 μm diamond suspension, and finished using Buehler MasterPrep 0.05 μm alumina suspension. The etching was performed using a 5% Nital solution for a period of 5 seconds. This etchant reveals only the microstructure of the base metal, but does not affect the surface alloyed layer. The surface alloyed layer was electro-etched using a solution of 85% ethanol and 15% HCl and passing a 2 Amp current through the electrode for a period of 1 minute. Kalling's Reagent 2 was used to reveal the grain boundaries of the surface alloyed layer.

Optical Microscopy

Optical microscopy was performed for microstructural study of the sample and to identify the phases present. It was to identify a ferritic (α-Fe) and pearlitic microstructure in the base metal. The Nikon Eclipse TS100 optical microscopes with Clemex Image Analysis software and ImageJ were used to investigate the microstructure of the surface alloyed samples.

Scanning Electron Microscopy And X-ray Diffraction

Scanning electron microscopy was used to is quantify the thickness of the interface, and energy-dispersive spectroscopy is used for chemical composition analysis of the samples. Backscatter mode was utilized to understand the distribution of the phases in the surface alloyed layer. JOEL JSM-6460 LV was the system utilized with the accelerating voltage being set at 15kV for SEM and EDS analysis. The EDS scan was aimed at quantifying the levels of Fe, Ni, Cr, Mn, and Mo in the surface alloyed samples. BSE was performed at an accelerating voltage of 20 kV on composition mode imaging.

Phase identification was carried out using a Bruker D8 Discover X-ray diffractometer (XRD). With the addition on ferrite (Ni) and austenite (Cr) stabilizers, it is expected to have both phases in the surface alloyed layer. Understanding the phase composition can help in developing appropriate heat treatment regimes.

Linear Polarization Test

Linear polarization testing was carried out to measure the corrosion current of the surface of the sample. The material is polarized during this test on the order of +/- 25 mV on an open-circuit potential, and the potential is measured when no net current is flowing. As the potential of the working electrode is changed, a current will be induced to flow between the working and counter electrodes, and the sample's resistance to polarization is found by taking the slope of the potential vs. current curve. The advantage of this test is that it is nondestructive, unlike the potentiodynamic polarization test, and it does not change the chemistry of the surface.

The samples were conditioned in an ASTM G61 3.56% saltwater solution for one hour and then underwent a linear polarization test for 10 minutes. A potentiostat, SP-200 BioLogic, was used to run the test. The electrolyte used for the corrosion test was 3.5% NaCl solution. The surface alloyed samples and graphite rod were used as the working electrodes and counter electrodes, respectively. For the reference electrode, Ag/AgCl electrode was used. After the test was completed, the corrosion current was extrapolated from the results of the experiment and was used to calculate the corrosion rate. To calculate the corrosion rate, the corrosion current must be changed to the corrosion current density, using the following equation

$$i_{corr} = \frac{I_{corr}}{A} \qquad \text{Eqn. 1}$$

where i_{corr} = corrosion current density ($\mu A/cm^2$), I_{corr} =

Table 2. Weight of Alloying Elements Used for the Surface Alloying of the Butterfly Valves

Sample	Binder medium	Ni (gm)	Cr (gm)	Fe–Mn (gm)	Fe–Si (gm)	Mo (gm)	Powder/area (gm/cm^2)
BV1	REFCOHOL 1010	0.51	1.19	–	–	–	0.106
BV2	REFCOHOL 1010	0.8	1.84	–	–	–	0.165
BV3	NaPA binder	0.56	2.19	0.11	0.12	0.30	0.205

total anodic current (μA) and A = exposed specimen area, cm^2

The equivalent weight is also needed to calculate the corrosion rate. The equivalent weight for each element and alloy is different, and the equation which follows shows how to calculate an equivalent weight for a pure material. The WCB equivalent weight was treated as a pure material because it consists of over 99% iron.

$$EW = \frac{W}{n} \quad \text{Eqn. 2}$$

where W = atomic weight of the element and n = the valance of the element

For an alloy, the equivalent weight must total the equivalent weights of each metal in the system and then must be added up and divided by 100. Below is the equation which details how to calculate equivalent the weight of an alloy

$$Q = \sum \frac{(n_i \times f_i)}{W_i} \quad \text{Eqn. 3}$$

where f_i=the mass fraction of the ith element in the alloy W_i=the atomic weight of the ith element in the alloy, and n_i=the valence of the ith element in the alloy.

The density (ρ, gm/cm^3) of the material must also be considered to calculate the corrosion rate. After calculating the necessary components for the corrosion rate equation, they can be substituted back into the equation for the corrosion rate, which is as follows,

$$CR = K_1 \times \left(\frac{i_{corr}}{\rho}\right) \times EW \quad \text{Eqn. 4}$$

CR is given in mm/year and i_{corr} is given in $\mu A/cm^2$.

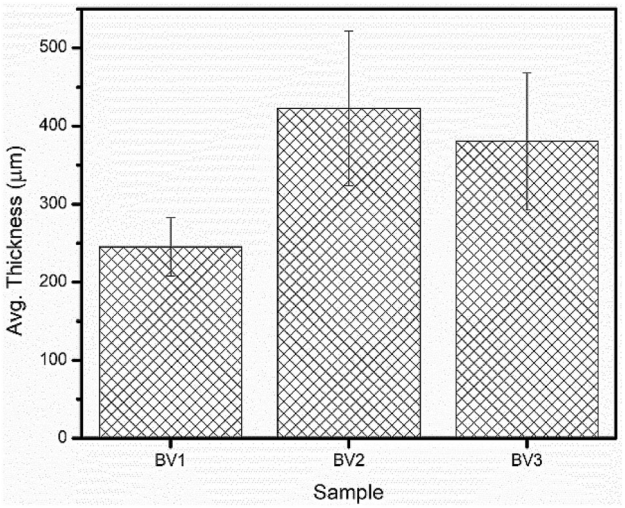

Figure 5. Average thickness of the surface alloyed layer in three castings of surface alloyed butterfly valves.

Results and Discussions

Microstructural and Phase Analysis

Optical micrographs of the cross section of surface alloyed as-cast samples are shown in Figure 4. A relatively uniform and continuous surface alloyed layer was observed in all samples. Occasional microporosity is observed in the surface alloyed layer. The average thickness of the surface alloyed layer is given in Figure 5.

Electro-etching of the surface alloyed layer was performed using an etchant made with 15% HCl and 85% ethanol and passing a 2 Amp current using an electrode placed on the surface alloyed layer. The base metal (Figure 6a) shows a ferrite and pearlite microstructure, which is typical of WCB steel. Figure 6b–d demonstrates the cross-sectional macro-morphology of the surface alloyed layer, indicating a surface alloyed layer free of cracks or porosity. The interface layer between the base metal and the surface alloyed layer does not show the presence of cracks.

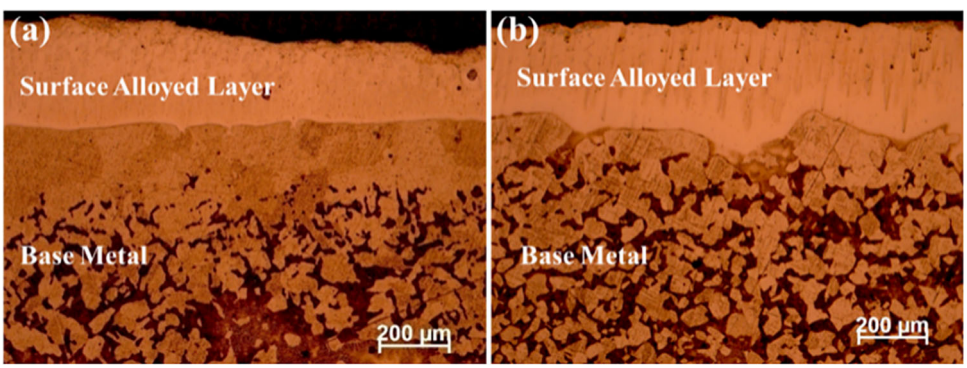

Figure 4. Optical images of the as-cast (a) BV1 and (b) BV2.

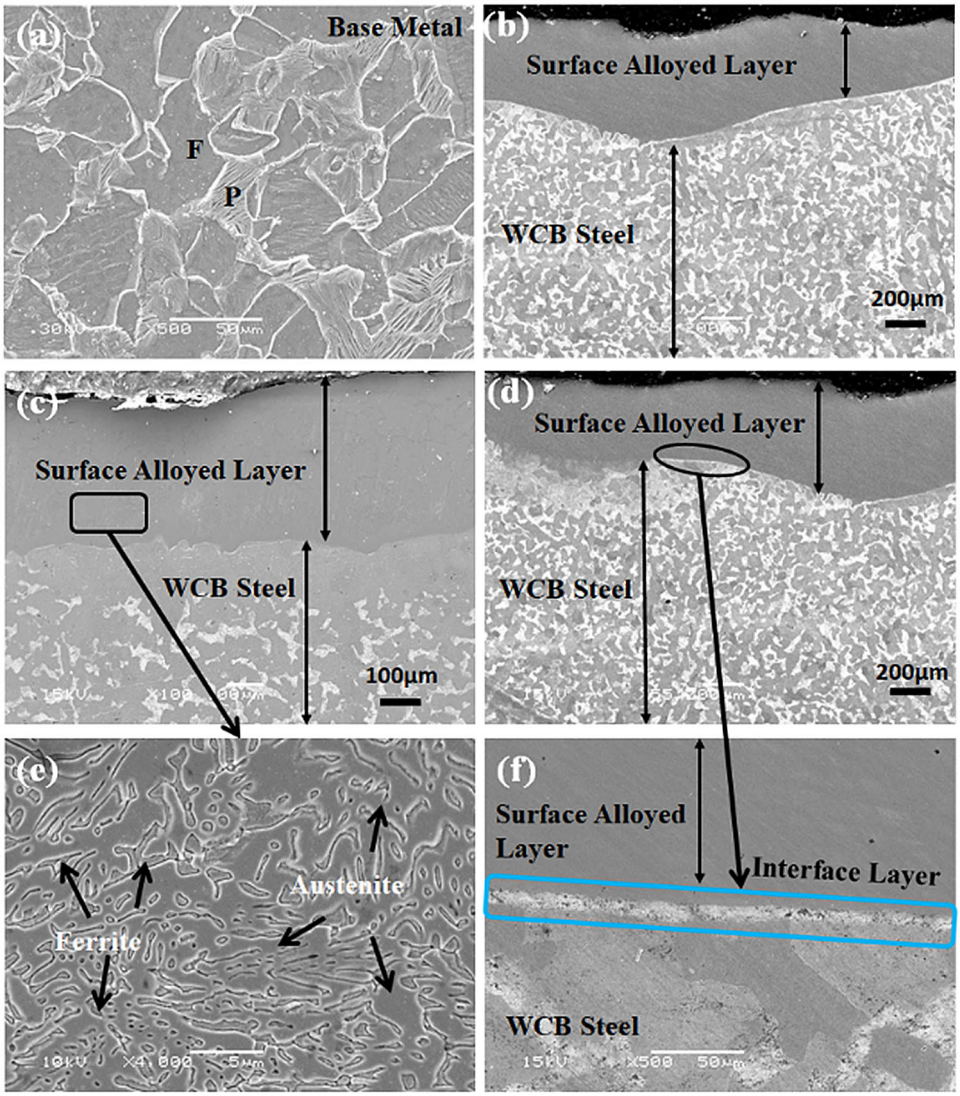

Figure 6. SEM micrograph of a base metal, (b d) BV1 surface alloyed layer, (c) BV2 surface alloyed layer in as-cast condition, (e) austenite–ferrite microstructure of the surface alloyed layer, (f) interface layer between surface alloyed layer and the base metal. All samples were in the as-cast condition.

The microstructure at the interface of the surface alloyed layer and the base metal suggests a good metallurgical bond. The microstructure in a typical surface alloyed layer (Figure 6e) is composed of austenite (γ) phases in the shape of elongated islands dispersed in the ferritic (α) matrix and free of precipitates. In addition, the morphology of the austenite phase ranged from elongated islands to an equiaxed form.

The EDS line scan results of surface alloyed sample BV3 (Figures 7) show the change in the gradient of various alloying element content from the substrate to the surface alloyed layer. Table 3 lists the composition of the surface alloyed layer and the interface. Compared with the original composition of the WCB steel, a significant increase of nickel, chromium, Mo, Mn, and Si has been detected in a surface alloyed layer. The analyses were performed in regions ferrite (α phase) and austenite (γ phase), indicated in the micrographs (Figure 6e). It was observed that the elements chromium and molybdenum are present in a higher percentage in the ferrite phase, since they are ferritizing elements, and nickel is present in a higher percentage in the austenite phase since it dissolves and stabilizes austenite.[13]

The dissolution of alloying elements added to the slurry coated on molds leads to the formation of the surface alloyed layer. The weight percentages of Ni and Cr drop at the interface while that of Fe increases sharply as one moves from the surface alloyed layer into the base substrate alloy, as shown in Figure 7. The area near the interface in the surface alloyed layer shows the lamellar structure (Figure 6b). The base metal retains its α and pearlite phase microstructure, and the region immediately

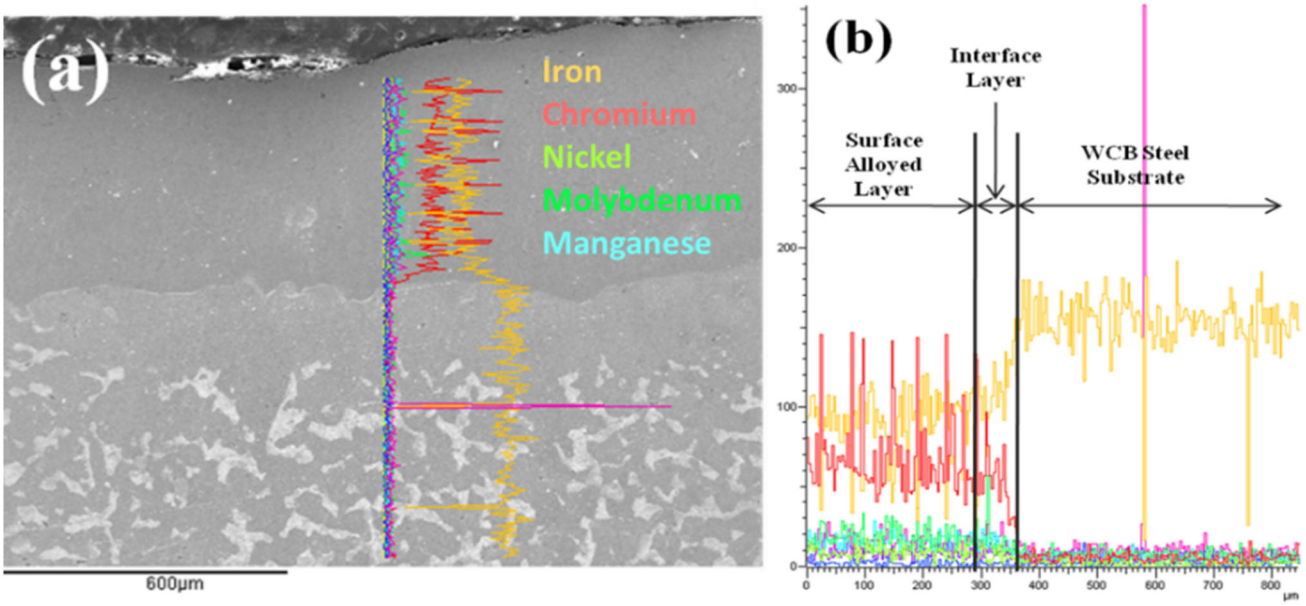

Figure 7. (a) Location of the EDS line scan on the cross section of the BV3 surface alloyed sample across the base metal and surface alloyed layer. (b) Plot of elemental intensity vs. distance in the EDS line scan.

Table 3. Chemical Composition of the Surface Alloyed Layer and Interface Layer in Sample BV3 (Table 2 as Determined Using Spark Spectrometer)

Elemental composition (in wt%)	Surface alloyed layer	Interface layer	WCB base metal
Cr	23.2	3.80	<0.5
Ni	6.4	3.89	<0.5
Mo	3.3	–	<0.2
Mn	1.1	1.04	<1
Si	0.7	0.54	0.6
Fe	Balance	Balance	Balance

below the interface shows primarily an α phase with some pearlite.

The XRD analysis of the surface alloyed layer of the surface alloyed sample BV3 is shown in Figure 8**.** It confirms the presence of ferrite, austenite, and chromium oxide (Cr_2O_3) in the surface alloyed layer. The presence of Cr_2O_3 is known to improve the corrosion resistance of the alloy. This oxide can form in ambient conditions; however, heat treatment of the alloy leads to the acceleration of the oxide formation. It should be noted that while there is a chance that all elements present in the system can form oxides (such as FeO, Fe_2O_3, Fe_3O_4, NiO) at high temperature, not all of these oxides can exist simultaneously in equilibrium with one another. The selective oxidation chromium can be explained by the standard free energy of formation and Ellingham's oxidation curve, as shown in Figure 9. It shows that Cr_2O_3 is more chemically stable than iron oxide

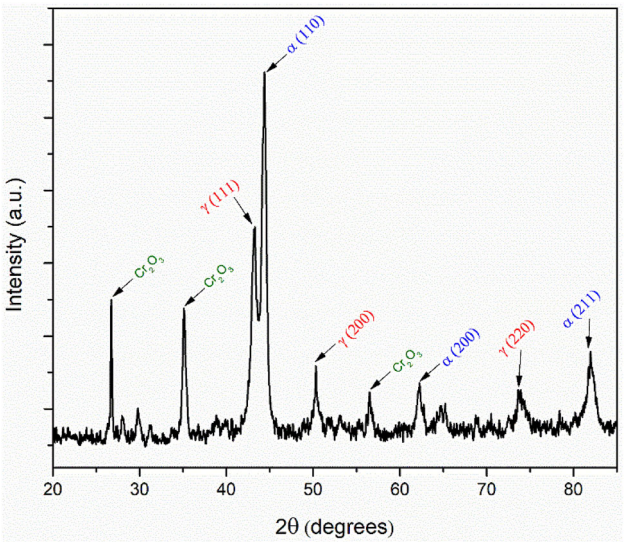

Figure 8. XRD analysis of the surface alloyed layer of the as-cast surface alloyed BV3 sample shows the presence of austenite (γ) and ferrite (α) as the primary phases in the surface alloyed layer.

and nickel oxide at all temperatures. The high degree of Cr_2O_3 peaks can be attributed to the high percentage of Cr (>23%) in the system.[14–16]

Hardness Measurements

The hardness of the surface alloyed layer and the base metal in the as-cast condition was measured using the Vickers microhardness test. The enrichment of the surface alloyed layer by alloying elements Ni, Cr, Mn, Si, and Mo

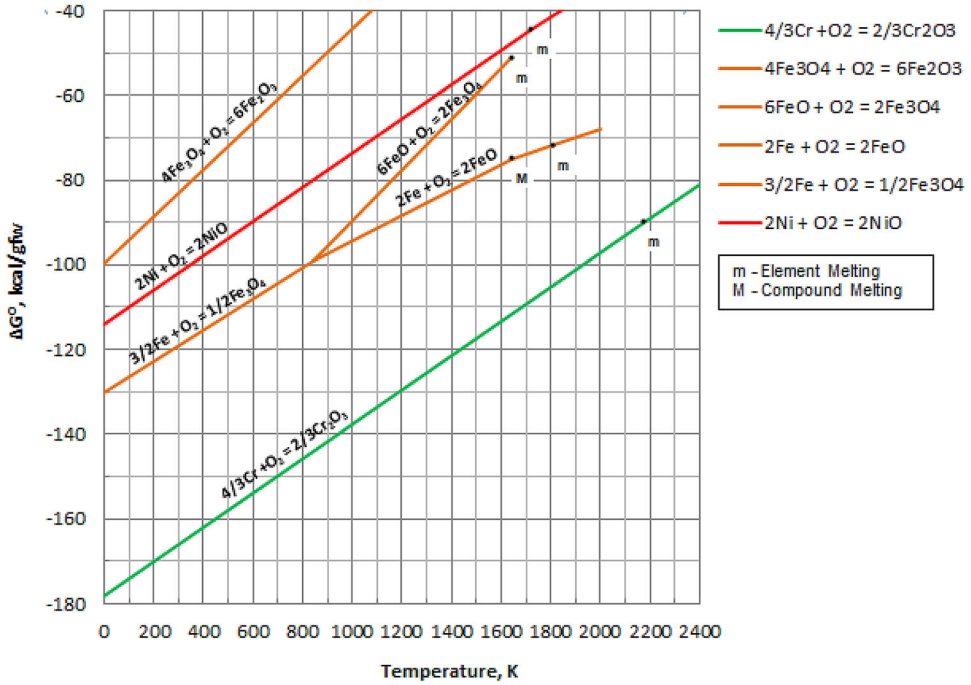

Figure 9. Ellingham diagram showing the free energy of the formation of oxides of various metals. The Cr_2O_3 line is highlighted in green in the diagram.[17]

led to an increase in the hardness of the surface alloyed layer. It has been previously reported by other researchers that the addition of Mo, Si, and Cr leads to an increase in the hardness, 0.2% proof stress, and tensile strength of the iron matrix.[18]

The samples were tested in an as-cast condition, with each sample undergoing multiple measurements through the cross section to ensure the average value is taken over the sample. The hardness measurements did not show any significant scatter within the surface alloyed layer, suggesting that the distribution of alloying elements in the surface alloyed layer is quite uniform (Figure 10).

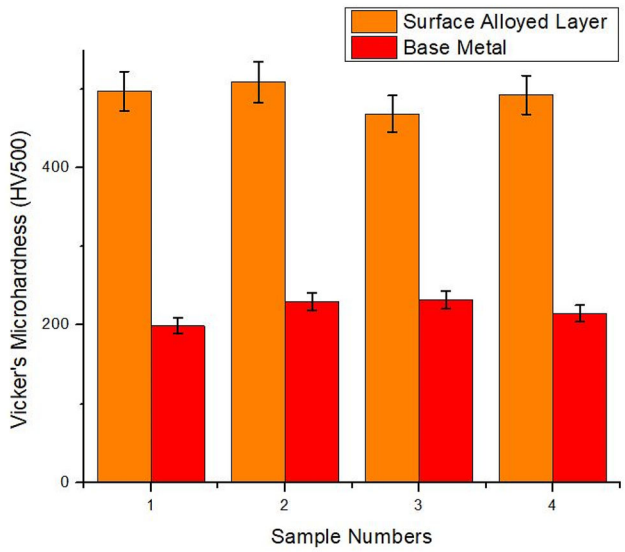

Figure 10. Comparison of the hardness of the surface alloyed layer and the base metal indicating a consistent increase in the as-cast condition.

Corrosion Resistance

There are two ways to improve the corrosion resistance of iron-based alloys: (1) to improve its thermodynamic stability by adding some alloying elements with higher thermodynamic stability like Ni and Cr to the solid solution to increase its electrode potential and to decrease the anodic activation and (2) to promote the formation of stable passivation on the surface and to improve its resistance on corrosion reaction by adding elements like Cr and Mo. Therefore, the large increases in the Ni and Cr content in the surface alloyed layers as a result of surface alloying can significantly improve its corrosion resistance. In addition, the rise in austenite in the microstructure of the alloyed layer will also improve the corrosion resistance. The fine

Table 4. Corrosion Rate Values for Surface Alloyed Samples and WCB

Sample	Corrosion rate (mm/year)
WCB base metal heat-treated (normalized and tempered)	0.12
Normalized and tempered surface alloyed sample BV1	0.06

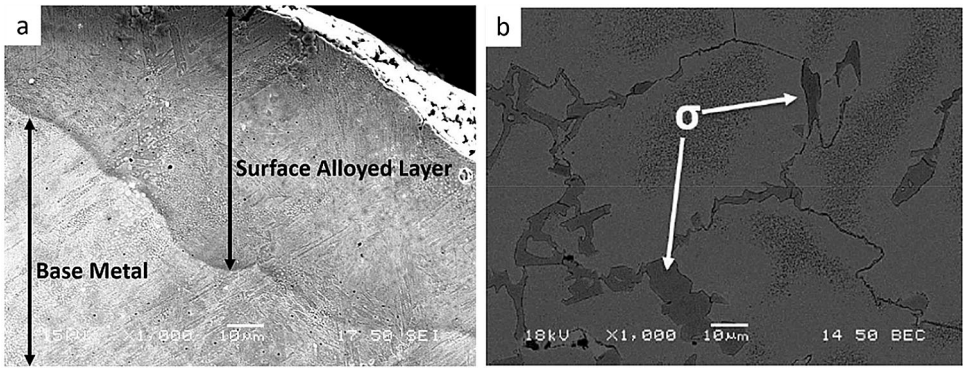

Figure 11. (a) The absence of the σ phase in the surface alloyed layer of surface alloyed sample BV3 after solution annealing at 850 C for a period of 100 seconds. (b) The presence of intermetallic σ phase in the surface alloyed layer of surface alloyed sample BV3 before heat treatment.

microstructure as a result of relatively rapid solidification in the surface alloyed layer segregation can also decrease the corrosion by the micro-cell effect.

Table 4 lists the corrosion rates of surface alloyed butterfly valves samples and the base WCB steel. From the table, it can be seen that the heat-treated (normalized and tempered) surface alloyed sample shows a half corrosion rate compared to heat-treated (normalized and tempered) WCB. The base metal WCB steel has a higher pearlite content, and it has been shown that there is accelerated galvanic corrosion between lamellar cementite and ferrite phase in pearlite banded structures.[19–25] Surface alloying and subsequent heat treatment transforms the microstructure to predominantly ferrite and austenite.

The as-cast microstructure of the surface alloyed layer showed the presence of intermetallic σ, which can be detrimental to the corrosion resistance of the surface alloyed layer. The solution annealing treatment led to the dissolution of the intermetallic phase, as shown in figure 11, which is expected to improve the corrosion resistance of the surface alloyed layer.

Applications

It has been demonstrated that the novel cast surface alloying process produces a surface alloyed layer enriched in several elements (including Ni, Cr, Mo, and Mn) on butterfly valve WCB steel sand castings. The surface alloyed WCB castings are slightly more expensive compared to WCB steel castings, but they are much lower in cost compared to through section stainless steel (as much as $10-12 per pound). The scalable and more economical techniques for coating sand molds and cores with a refractory wash containing metal and ferroalloy powder for surface alloying could include flow coating, spray coating, dipping, and brush coating.

This demonstrates the potential of reducing production costs of using surface alloyed WCB steels compared to through section stainless steel components. It also demonstrates that surface alloyed steel castings provide much more improved corrosion resistance, with only a marginal increase in the cost over plain WCB steel castings. This suggests several other potential applications of surface alloyed WCB castings in addition to butterfly valves, where corrosion and wear resistance higher than that of WCB steel are required.

Conclusions

The WCB steel butterfly valve sand castings were successfully surface alloyed with Ni, Cr, Mn, Si, and Mo by adding powders of nickel, chromium, ferrosilicon, ferromanganese, and molybdenum to the mold coating. The surface of the WCB steel butterfly valve casting was enriched with up to 23.2 weight % Cr, 6.4 weight % Ni, 1.1 weight % Mn, and 3.3 weight% Mo, during sand casting as a result of mixing of nickel, chromium, ferromanganese, and molybdenum powders to mold coatings. Austenite and ferrite were the primary phases observed in the as-cast surface alloyed layer. Samples from normalized and tempered surface alloyed butterfly valve castings made in this study are likely to exhibit a 50% decrease in corrosion rate as compared to base metal WCB steel, as suggested by the linear polarization test conducted in this study. The surface alloyed WCB alloy castings are likely to have much higher wear resistance, as suggested by the higher hardness of the surface alloyed layer on the castings.

The following areas require further work: developing quantitative relationships between processing parameters and the thickness, composition, phase structure, residual stresses, adhesion, surface finish of surface alloyed layers, and their influence on corrosion and hardness. The mechanisms of melting and dissolution of powders in mold coatings, formation of optimum solidification

microstructures, and the effect of post-casting heat treatments need to be further studied as well.

Acknowledgements

The authors thank NSF WEP IUCRC for funding the project under the grant number 1540032. The authors express their gratitude to their industrial partner, Badger Alloys Inc., for casting prototypes of surface alloyed butterfly valves.

REFERENCES

1. J. R. Davis, *Alloying Understanding the Basics*. (ASM International, Geauga County, 2001).
2. X. Jiang, A. Jiahe, X. Xie, Z. Xu, Multi-element Ni–Cr–Mo–Cu surface alloyed layer on steel using a double glow plasma process. Surf. Coat. Technol. **168**(2), 142–147 (May 2003). https://doi.org/10.1016/S0257-8972(03)00008-2
3. S. Anandan, S. Pityana, and J. Dutta Majumdar, Structure–property-correlation in laser surface alloyed AISI 304 stainless steel with WC+Ni+NiCr. Mater. Sci. Eng. A, **536**, 159–169. Doi: https://doi.org/10.1016/j.msea.2011.12.095.
4. M. Krishnakumar, R. Saravanan, Surface alloying on austenitic stainless steel with titanium and tungsten using gas tungsten arc. Eng. Res. Express **1**(2), 025005 (Oct. 2019). https://doi.org/10.1088/2631-8695/ab47b5
5. H.C. Fals, A.S. Roca, J.B. Fogagnolo, L. Fanton, M.J.X. Belém, C.R.C. Lima, Erosion–corrosion resistance of laser surface alloying of NbC thermal spray coatings on AISI 304L steel. J. Therm. Spray Tech. **29**(1), 319–329 (Jan. 2020). https://doi.org/10.1007/s11666-019-00973-y
6. N. Jeyaprakash, C.-H. Yang, S. Sivasankaran, Laser cladding process of cobalt and nickel based hard-micron-layers on 316L-stainless-steel-substrate. Mater. Manuf. Process. **35**(2), 142–151 (Jan. 2020). https://doi.org/10.1080/10426914.2019.1692354
7. A. Amirsadeghi, M.H. Sohi, Comparison of the influence of molybdenum and chromium TIG surface alloying on the microstructure, hardness and wear resistance of ADI. J. Mater. Process. Technol. **201**(1–3), 673–677 (2008)
8. L. Jinlong, L. Tongxiang, W. Chen, Surface enriched molybdenum enhancing the corrosion resistance of 316L stainless steel. Mater. Lett. **171**, 38–41 (2016)
9. B.N. Mordyuk, G.I. Prokopenko, PYu. Volosevich, L.E. Matokhnyuk, A.V. Byalonovich, T.V. Popova, Improved fatigue behavior of low-carbon steel 20GL by applying ultrasonic impact treatment combined with the electric discharge surface alloying. Mater. Sci. Eng. A **659**, 119–129 (Apr. 2016). https://doi.org/10.1016/j.msea.2016.02.036
10. L. Song, G. Zeng, H. Xiao, X. Xiao, S. Li, Repair of 304 stainless steel by laser cladding with 316L stainless steel powders followed by laser surface alloying with WC powders. J. Manuf. Process. **24**, 116–124 (Oct. 2016). https://doi.org/10.1016/j.jmapro.2016.08.004
11. H.T. Cao, X.P. Dong, Z. Pan, X.W. Wu, Q.W. Huang, Y.T. Pei, Surface alloying of high-vanadium high-speed steel on ductile iron using plasma transferred arc technique: Microstructure and wear properties. Mater. Des. **100**, 223–234 (Jun. 2016). https://doi.org/10.1016/j.matdes.2016.03.114
12. D. F. Macdonald, Process of coating metal castings US3450189A. Jun 17, 1969.
13. S. C. de Rezende, I. Dainezi, R. C. Apolinario, L. L. de Sousa, and N. A. Mariano, "Influence of Molybdenum on microstructure and pitting corrosion behavior of solution-treated duplex stainless steel in a lithium chloride solution. Mater. Res. **22**, 2019.
14. T. Ohmi, Y. Nakagawa, M. Nakamura, A. Ohki, T. Koyama, Formation of chromium oxide on 316L austenitic stainless steel. J. Vac. Sci. Technol. A **14**(4), 2505–2510 (Jul. 1996). https://doi.org/10.1116/1.580010
15. H.J.T. Ellingham, Reducibility of oxides and sulphides in metallurgical processes. J. Soc. Chem. Ind. **63**(5), 125–133 (1944)
16. F.D. Richardson, J.H.E. Jeffes, Free energies of formation of metal oxides as a function of temperature. J. Iron Steel Inst. **160**, 261–273 (1948)
17. M. Hasegawa, Ellingham diagram in *Treatise on Process Metallurgy* (Elsevier, London, 2014). pp. 507–516.
18. N. Ohkubo, K. Miyakusu, Y. Uematsu, H. Kimura, Effect of alloying elements on the mechanical properties of the stable austenitic stainless steel. ISIJ Int. **34**(9), 764–772 (1994)
19. C.X. Shan, X. Hou, K.-L. Choy, Corrosion resistance of TiO2 films grown on stainless steel by atomic layer deposition. Surf. Coat. Technol. **202**(11), 2399–2402 (Feb. 2008). https://doi.org/10.1016/j.surfcoat.2007.08.066
20. N.C. Hosking, M.A. Ström, P.H. Shipway, C.D. Rudd, Corrosion resistance of zinc–magnesium coated steel. Corros. Sci. **49**(9), 3669–3695 (Sep. 2007). https://doi.org/10.1016/j.corsci.2007.03.032
21. P. Jayaweera, D.M. Lowe, A. Sanjurjo, K.H. Lau, L. Jiang, Corrosion-resistant metallic coatings on low carbon steel. Surf. Coat. Technol. **86–87**, 522–525 (Dec. 1996). https://doi.org/10.1016/S0257-8972(96)03087-3
22. M. Dutta, A.K. Halder, S.B. Singh, Morphology and properties of hot dip Zn–Mg and Zn–Mg–Al alloy coatings on steel sheet. Surf. Coat. Technol. **205**(7), 2578–2584 (Dec. 2010). https://doi.org/10.1016/j.surfcoat.2010.10.006

23. A. Wiengmoon, J.T.H. Pearce, T. Chairuangsri, Relationship between microstructure, hardness and corrosion resistance in 20wt.%Cr, 27wt.%Cr and 36wt.%Cr high chromium cast irons. Mater. Chem. Phys. **125**(3), 739–748 (Feb. 2011). https://doi.org/10.1016/j.matchemphys.2010.09.064
24. R. W. Revie, *Corrosion and corrosion control: an introduction to corrosion science and engineering*. (John Wiley & Sons, London, 2008).
25. S. K. Behera, A. Kumar P, N. Dogra, M. Nosonovsky, and P. Rohatgi, Effect of Microstructure on Contact Angle and Corrosion of Ductile Iron: Iron–Graphite Composite. *Langmuir*, **35**(49), 16120–16129, Dec. 2019. doi: https://doi.org/10.1021/acs.langmuir.9b02395.

Publisher's Note Springer Nature remains neutral with regard to jurisdictional claims in published maps and institutional affiliations.